Intermetallics 56 (2015) 96–100

Contents lists available at ScienceDirect

Intermetallics

journal homepage: www.elsevier.com/locate/intermet

# Dynamic fragmentation induced by network-like shear bands in a Zr-based bulk metallic glass

F. Zeng [a], Y. Chen [a], M.Q. Jiang [a], C. Lu [b], L.H. Dai [a, c, *]

[a] State Key Laboratory of Nonlinear Mechanics, Institute of Mechanics, Chinese Academy of Sciences, Beijing 100190, China
[b] Department of Mechanical Engineering, Curtin University, Perth, WA 6845, Australia
[c] State Key Laboratory of Explosion Science and Technology, Beijing Institute of Technology, Beijing 100081, China

ARTICLE INFO

*Article history:*
Received 20 May 2014
Received in revised form
12 August 2014
Accepted 14 September 2014
Available online 3 October 2014

*Keywords:*
A. Metallic glasses
B. Elastic properties
B. Fracture
B. Shear band

ABSTRACT

Dynamic fragmentation induced by network-like shear bands is observed in a Zr-based bulk metallic glass subjected to impact loading, which is different from shear failure via one dominant shear band under quasi-static compression. Further, the influence of elastic strain energy on the evolution of shear bands is investigated. It is shown that the shear-band pattern occurring in one dominated mode or in multiple modes strongly depends on the loading rates. Dynamic fragmentation is due to the competition between the elastic strain energy driving a shear band and the dissipated energy along the shear band.


## 1. Introduction

A fundamental understanding of fragmentation of solids under impulsive loading is important in aerospace, military and civil industries. Cracks as the basic source of fragmentation originate from inherent flaws or adiabatic shear bands during dynamic loading [1–8]. Generally speaking, dynamic fragmentation of brittle materials (rocks, glasses and ceramics) such as in plate impact tests is resulted from the nucleation and propagation of numerous flaw-induced cracks [1–4]. However, cracks initiating in adiabatic shear bands may also lead to fragmentation of ductile crystalline metals in cylinder exploding tests [5–8]. These experimental phenomena imply that there are some potential relationships between fragmentation and the macroscopic plasticity in brittle or ductile materials.

Bulk metallic glasses (BMGs), as an emerging class of materials, are usually the lack of global ductility like traditional brittle solids, but their atoms are densely packed with cohesive metallic bonds similar to crystalline metals [9–17]. This unique combination may lead to an abnormal mechanism of fragmentation. According to recent studies by Tandaiya et al. [18,19], crack initiates and then stably grows inside one dominant shear band in bending tests of BMGs with a notch, which shows that shear bands are precursors of cracks. Fracture of Zr-based BMGs into a few fragments has been discovered in split-Hopkinson pressure bar [20,21] and anvil-on-rod impact tests [12,22]. The typical vein pattern [23,24] observed on fragments indicates that there is a correlation between structural disorder induced shear bands [25–29] and macroscopic fragmentation [12,20–22] in BMGs. However, the underlying physics that dominates fragmentation of BMGs still remains elusive.

Since crystalline or amorphous alloys are prone to shear banding, the mechanism of flow localization has been discussed in the viewpoint of mechanical diffusion [1,6,16,25–31]. But, in addition to thermal and momentum diffusions, metallic glasses involve free-volume diffusion due to their abnormal atomic structures. Shear banding in BMGs is a consequence of the balance between free-volume diffusion and free-volume creation driven by shear stresses [16,28,32,33]. The free-volume diffusion determines the thickness of a shear band [26,27,33]. Thermal and momentum diffusions that are out of a shear band and into its neighbouring medium can produce a heat-affected zone [34,35] and a momentum diffusion zone or shear-band spacing [25,36,37], respectively.

Recently, theoretical efforts have been made to understand the evolution of shear bands. For example, combining the momentum

* Corresponding author. State Key Laboratory of Nonlinear Mechanics, Institute of Mechanics, Chinese Academy of Sciences, Beijing 100190, China. Tel.: +86 10 82543931; fax: +86 10 82543977.
*E-mail address:* lhdai@lnm.imech.ac.cn (L.H. Dai).

http://dx.doi.org/10.1016/j.intermet.2014.09.008
0966-9795/

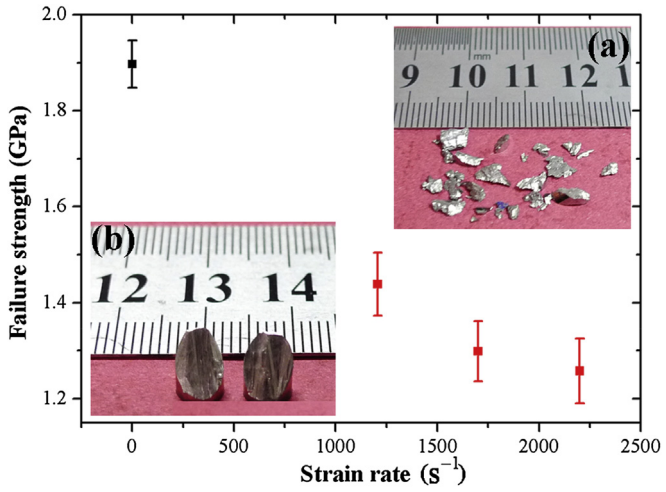


**Fig. 1.** Dependence of the failure strength on strain rates, where insets indicate (a) fragments under dynamic compression and (b) shear failure under quasi-static compression, respectively.

diffusion model firstly proposed by Grady and Kipp [31] with the free-volume and heat evolution, the evolution features of shear bands (e.g., shear-band toughness, thickness and spacing) [25,26,37,38] were investigated. In these studies, a rigid–plastic assumption was applied and thus the influence of elastic strain energy on shear banding is disregarded. As is well known, however, shear banding in solids can be considered as a dissipation system [1,6,16,25,26,37,38], and elastic strain energy contributes to shear localization [39]. In particular, since the localized plastic flow in BMGs is concentrated in a rather thin shear band surrounded by an elastically deformed matrix, the elastic strain energy cannot be ignored. In this paper, fragmentation of a Zr-based BMG under impact loading is observed and the influence of elastic strain energy on the shear-band evolution is studied. Based on experimental observations and an evolution model of shear bands, the underlying mechanism of dynamic fragmentation in BMGs is unveiled.

## 2. Experimental procedure and results

In experiments, $Zr_{41.2}Ti_{13.8}Cu_{10}Ni_{12.5}Be_{22.5}$ (Vit 1) BMGs were adopted and their glassy nature was confirmed by the X-ray diffraction. Specimens with 7.5 mm in length and 5 mm in diameter were tested under quasi-static and dynamic compressions with an applied strain rate ranging from $10^{-4}$ to $10^{3}$ $s^{-1}$. The quasi-static compression was performed on the MTS-810 material testing machine with a fixed strain rate of $1 \times 10^{-4}$ $s^{-1}$ and dynamic compression was carried out on the split-Hopkinson pressure bar apparatus with strain rates from $1 \times 10^{3}$ to $2.5 \times 10^{3}$ $s^{-1}$.

Under dynamic compression, Vit 1 BMGs break into many small fragments as shown in Fig. 1a, and while under quasi-static loading they fracture along a single shear band (see Fig. 1b). It is obvious that the failure strength monotonically decreases with the increase of strain rates, consistent with other Zr-based BMGs [11,12,21]. Typical scanning electron microscope images of fracture surface are given in Fig. 2. In the case of quasi-static loading, uniformly distributed vein patterns are observed on the whole fracture surface (Fig. 2a and b), indicating that fracture is dominated by one shear band. However, under dynamic compression, randomly distributed vein patterns are seen on the surface of a fragment (Fig. 2c and d), which implies that fragments are generated by shearing on multiple planes.

As shown in Fig. 3, there are multiple shear bands on the surface of a fragment, involving uniform and wavy primary and secondary ones (indicated by red and black arrows, respectively) in different directions. The distances between two wavy bands are about 30–50 μm and 3–15 μm, corresponding to primary and premature shear bands respectively, and their interaction constructs a network-like deformation zone. Once the shear displacements on some shear bands reach their critical values, cracks initiate, propagate and ultimately lead to fragmentation. Thus, the size of

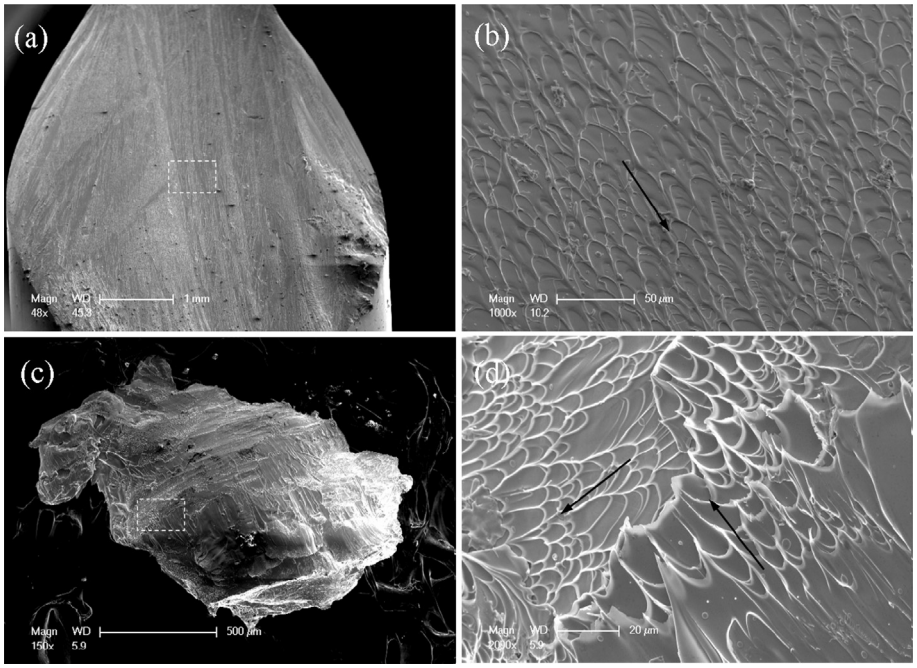


**Fig. 2.** Scanning electron microscope images of failure modes, where (a) and (b) are the fracture surface of a sample and uniformly distributed vein patterns under quasi-static compression, and (c) and (d) are the fragment topography and vein patterns with multiple directions under dynamic compression.

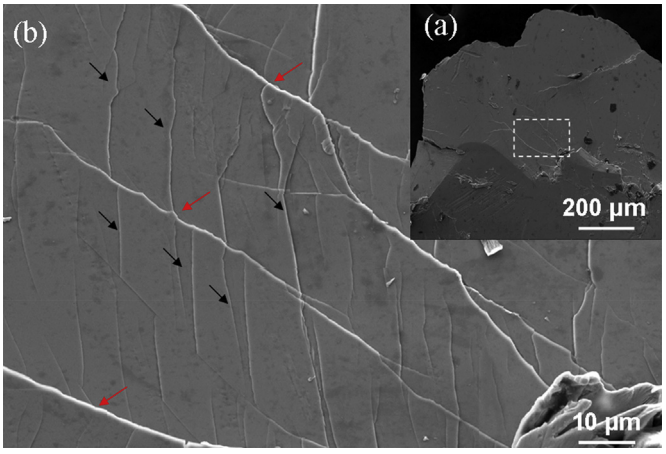


**Fig. 3.** Scanning electron microscope image on a fragment surface under dynamic loading and (b) its enlarged network-like shear bands in the squared area. (For interpretation of the references to colour in this figure legend, the reader is referred to the web version of this article.)

fragments (see Fig. 1a) is usually much larger than the spacing of shear bands. Generally, shear bands are predecessors of cracks, and hence failure of BMG samples is due to shear banding. Here the key issue is on the formation and evolution of network-like shear bands that lead to dynamic fragmentation of BMGs, which is in contrast to a single primary shear band in quasi-static fracture. Obviously, whether the shear-band pattern occurs in one dominated mode or multiple modes strongly depends on strain rates.

## 3. Theoretical analysis and discussion

BMG samples do not undergo a full-field global plastic deformation when subjected to dynamic loading at room temperature. Instead, yielding preferentially occurs in some regions via a local rearrangement of atoms such as shear transformation or atomic jumps, forming local plastic regions. In these regions, shear bands nucleate and propagate. As mentioned above, shear banding in metallic glasses can be regarded as a dissipation system in which the elastic strain energy is dissipated through plastic deformation in shear bands and their growth to form shear cracks. Some earlier works have indicated that the plastic deformation in shear bands is main dissipation source. For example, the applied energy is spent in plastic flow mediated by multiple shear bands when BMGs are subjected to bending [25,36]. Ductile metallic glasses with high fracture toughness is also due to the activities of shear bands in terms of multiplication, branching and intersection, ahead of a notch tip [40]. From the energetic viewpoint, the multiplication of shear bands is triggered when one shear band is not enough to dissipate the applied elastic strain energy. Therefore, it is important to investigate the competition between the dissipated energy and elastic strain energy during shear banding.

As illustrated in Fig. 4(a) and (b), at the time $t = 0$, the BMG is shearing at a local strain rate of $\dot{\gamma}_l$ along the $x$ direction, which yields at the shear stress $\tau_y$. Here, a shear band is assumed to initiate on the plane $y = 0$. During the shear-band propagation, the local redistribution of momentum is associated with the inertial effect. The momentum diffusion spreading out of the shear band and into its neighbouring medium would produce an elastic zone due to stress-relaxation from the shear band. Such a zone locates between the shear band and the local plastic region, where an elastic–plastic interface is at the position of $y = \zeta$, as shown in Fig. 4b. The dissipated energy within the shear band progressively increases as deformation evolves. At a time of $t = t_c$, the shear band is regarded as being fully matured and the dissipated energy reaches a critical level. Here, let us focus on a mature shear band and consider the critical dissipated energy in it. Based on the momentum diffusion mechanism, a theoretical model with the assumption of a rigid–plastic material was proposed to describe shear banding by Jiang and Dai [26]. In their analysis, the momentum, energy and free-volume balance was taken into account, including the primary free-volume softening mechanism of shear bands in BMGs. Here, it is worth noting that elasticity does not affect the energy dissipation in a shear band [26,30,31]. Then an expression can be derived that relates the critical dissipated energy to a structural disorder state within the mature shear band [26], that is

$$\Gamma_c = \left(\frac{9\rho D^3 \xi_c^6 \tau_y^3}{\dot{\gamma}_l R^5}\right)^{1/4}, \tag{1}$$

where $\Gamma_c$ is the energy per unit area, $\rho$ is the density, $D$ is the diffusion coefficient of free-volume, $\xi_c$ is the increase of free-volume concentration within a shear band, and $R$ is the local dilatation.

In previous analysis on the evolution of a shear band [25,26,37,38], a rigid–plastic assumption in BMGs was usually introduced and the elastic strain energy was omitted. As shown in Fig. 4b, however, there is an elastic region and the energy in Eq. (1) is supplied by elastic strain energy stored in the region. Here it is assumed that the elastic strain energy is fully released during shear banding, and thus we have

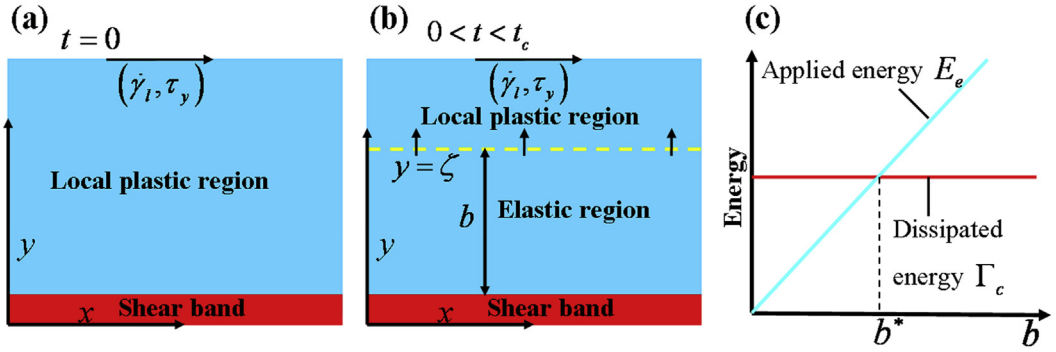


**Fig. 4.** Schematic of the shear-band evolution at (a) its initial and (b) evolving stages. (c) Illustration of the competition between the critical energy dissipated within a shear band and the applied energy near it.

$$E_e = \frac{\tau_y^2}{2\mu} b, \tag{2}$$

where $E_e$ is the elastic energy per unit area, $\mu$ is the elastic shear modulus, and $b$ is the normal distance from a shear band. In general, under a fixed loading condition, the energy in Eq. (1) is approximately a constant. However, the available strain energy linearly increases with the distance $b$ in Eq. (2), as shown in Fig. 4c. These two energies are equal and balanced at a distance of $b^*$. In the case of $b$ being less than or equal to $b^*$, one shear band would dominate shear failure. On the other hand, in the case of $b > b^*$, additional shear bands would form that construct a network-like configuration. For example, as shown in Fig. 3b, the two families of shear bands lead to dynamic fragmentation. Therefore, in both cases, the elastic strain energy as a function of $b$ determines the shear-band pattern and failure mode. Further analysis will reveal that there is an intrinsic relationship between $b$ and the momentum diffusion distance, and that the elastic strain energy in the momentum diffusion zone is fully released to drive the growth of a shear band in BMGs under impact loading.

As illustrated in Fig. 4b, during the shear-band evolution, the elastic region with a width of $\zeta$ is produced, and the velocity $V_\zeta = \dot{\gamma}_l \zeta$ along the $x$ direction on its upper boundary is controlled by the momentum diffusion. Let us approximately consider the elastic region as a whole, and thus its velocity field is given by $V = \dot{\gamma}_l \zeta$. Then, the time derivative of the momentum in the region can be calculated by

$$\tau_y - \tau_0 = \rho \dot{\gamma}_l \int_0^{\zeta} \dot{\zeta} \mathrm{d}x, \tag{3}$$

where $\tau_y$ and $\tau_0$ are shear stresses on its upper and lower boundaries, respectively, and $\dot{\zeta}$ is the velocity of the elastic–plastic interface along the $y$ direction. Under a simplified assumption of linear elastic unloading, the elastic strain energy that contributes to shear banding in the region is obtained as

$$E_r = \left(1 - \frac{\tau_0^2}{\tau_y^2}\right) E_e, \tag{4}$$

where $\tau_0/\tau_y$ indicates the proportion of released elastic strain energy in the total stored energy. In Eq. (3), the material properties of Vit 1 BMG are $\tau_y = 1$ GPa, $\rho = 6125$ kg m$^{-3}$ and $\dot{\zeta} = 2400$ m s$^{-1}$ (the elastic shear wave speed). As the shear band is matured, the momentum diffusion stops and its transport distance $\zeta$ is equal to the shear-band spacing [26,30,31], which roughly ranges from 1 to 100 μm [9–15] and is sensitive to the loading mode [41,42], sample geometry [36] and material composition [43]. According to experimental observations, we choose the spacing as in the order of 50 μm. The local strain rate $\dot{\gamma}_l$ could reach ~$10^7$ s$^{-1}$ or higher in dynamic indentation [37,38]. Thus, the corresponding local strain rate is approximately $10^7$ s$^{-1}$ at a macroscopic loading rate of $10^3$ s$^{-1}$. Applying these estimated parameters to Eq. (3), we have $\tau_0/\tau_y \approx 0$ under dynamics loading. Then, substituting it into Eq. (4), it is shown that, as a BMG is subjected to dynamic loading, the elastic strain energy within the momentum diffusion zone is almost fully released to drive shear banding, indicating that $b$ is equal to the shear-band spacing. However, there is no such a relationship for BMGs under quasi-static loading.

According to Eq. (3), the local strain rate $\dot{\gamma}_l$ is a key variable. In quasi-static tests (with a macroscopic strain rate of $10^{-4}$ s$^{-1}$), $\dot{\gamma}_l$ could be as high as $10^3$ s$^{-1}$ [28,37]. Therefore, we have $\tau_0/\tau_y \approx 1$ in the case of $\dot{\gamma}_l = 10^3$ s$^{-1}$. This implies that elasticity is not influenced by the inertial effect and the elastic strain energy within a momentum diffusion region is not a source of shear localization. For BMGs under quasi-static loading, however, the elastic strain energy near a shear band is affected by softening from localized flow. The energy within a heat-affected zone is released to fuelling shear banding.

The free-volume, heat and momentum diffusions control the three kinds of band-like structures, respectively [16,26,28]. In the case of free-volume diffusion, the width of a shear band is related to the critical time $t_c$ and $\delta_B \approx (Dt_c)^{1/2}$ [16]. The spacing of shear bands $\Delta \approx \sqrt{(\tau_y/\rho\dot{\gamma}_l)t_c}$ is equal to the transport distance of momentum diffusion [30,31], and the width of a heat-affected zone is given by $\delta_H \approx (\chi t_c)^{1/2}$ [42], with $\chi$ the heat diffusion coefficient. Eliminating the critical localization time, we have two relationships among these three band-like structures, that is, $\Delta \approx \delta_B \sqrt{(\tau_y/\rho\dot{\gamma}_l)/D}$ and $\delta_H \approx \delta_B(\chi/D)^{1/2}$. Thus, to drive a shear-band process the unit-area, elastic strain energy in a heat-affected zone under quasi-static compression is obtained as

$$E_{es} = \frac{\tau_{ys}^2 \delta_B}{2\mu} \sqrt{\frac{\chi}{D}}, \tag{5}$$

and similarly, the elastic strain energy in a momentum diffusion zone under dynamic compression is.

$$E_{ed} = \frac{\tau_{yd}^2 \delta_B}{2\mu} \sqrt{\frac{\tau_{yd}}{\rho\dot{\gamma}_l D}}, \tag{6}$$

where $\delta_B = 10$ nm [16], $D = 5 \times 10^{-9}$ m$^2$ s$^{-1}$ [26], $\chi = 3.0 \times 10^{-6}$ m$^2$ s$^{-1}$ [35], and $\mu = 35.3$ GPa for Vit 1 BMGs. As shown in Fig. 1, the quasi-static failure strength of 1.9 GPa is corresponding to the shear yield strength $\tau_{ys} = 0.95$ GPa. For simplification, the dynamic failure strength of 1.4 GPa is chosen, which is between 1.6 and 1.2 GPa (see Fig. 1), and thus the dynamic shear strength is $\tau_{yd} = 0.7$ GPa. Other relevant parameters are $R = 0.0027$ [44] and $\xi_c = 4\%$ [17]. According to Zhang et al. [37], the local strain rate $\dot{\gamma}_l$ from $10^3$ to $10^9$ s$^{-1}$ covers macroscopic quasi-static and dynamic loading rates. So the local strain rate $\dot{\gamma}_l = 10^6$ s$^{-1}$ can be considered as a transition from quasi-static to dynamic loading.

As shown in Fig. 5, the influence of elastic strain energy on the transition of failure modes from shear fracture to fragmentation can be clarified based on Eqs. (1), (5) and (6). For BMGs subjected to

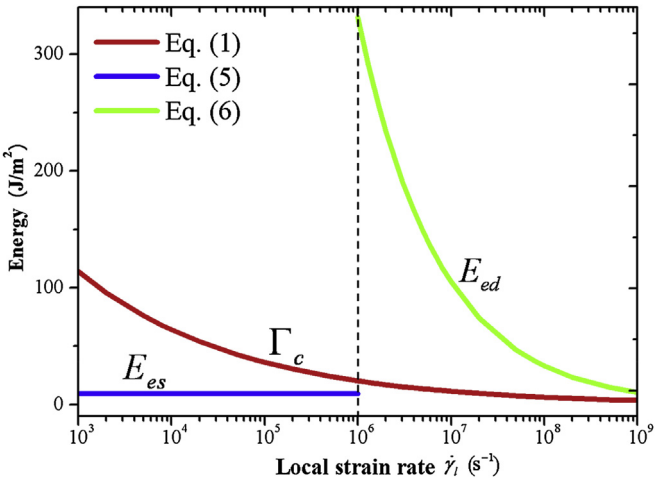


**Fig. 5.** The critical dissipation energy ($\Gamma_c$) in a shear band and strain energies ($E_{ed}$ and $E_{es}$) in momentum diffusion and heat-affected zones as a function of the local strain rate. The dashed line represents a transition from quasi-static to dynamic loading.

dynamic loading, since the strain energy from a momentum diffusion zone is more than the critical dissipation energy within one shear band, i.e., $E_{ed} > \Gamma_c$, fragmentation induced by network-like shear bands occurs. In contrast, under quasi-static loading, the critical dissipation energy is more than the strain energy from a heat-affected zone, indicating that one shear band is sufficient enough to dissipate the applied energy and then shear fracture occurs.

In our model, the stored energy is mainly dissipated by plastic deformation in multiple shear bands. Actually, there are two dissipation sources in the shear-band propagation and crack extension. According to quasistatic testing of four-point-bend notched BMGs by Tandaiya et al. [19], the estimated energy release rate under mode II is $J_c = 8.4$ N mm$^{-1}$. In their work, $J_c$ mainly contributes to the specific work of separation during a stable crack extension. Here, we consider that the dissipated energy in a crack extension is approximately equal to $J_c$. In the case of quasi-static loading, the shear-band dissipation energy, $\Gamma_c \sim (110 - 30)$ N mm$^{-1}$, is obtained by Eq. (1), which is much larger than $J_c$. Such a relationship is also expected for dynamic loading case. Thus, it is reasonable for us to consider shear bands (plastic deformation) as the main dissipation source.

## 4. Conclusions

In summary, dynamic fragmentation induced by network-like shear bands is observed in a Zr-based BMG under impact loading, which is in contrast to shear failure controlled by one dominated shear band. To understand this phenomenon, a theoretical model is proposed that takes into account the influence of elastic strain energy on the shear-band evolution. It is shown that, with the increase of strain rates, shear-band patterns transfer from one dominated mode to multiple modes. Dynamic fragmentation is due to the competition between the energy dissipated within a shear band and the elastic strain energy in a momentum diffusion zone. The good agreement between experimental observations and theoretical analysis indicates that the elastic strain energy plays an important role in shear banding.

## Acknowledgements

The work is supported by the National Natural Science Foundation of China (Grant Nos. 11472287, 11132011 and 11202221), the National Basic Research Program of China (Grant No. 2012CB937500), and the CAS/SAFEA International Partnership Program for Creative Research Teams.

## References

[1] Meyers MA. Dynamic behavior of materials. London: John Wiley & Sons; 1994.
[2] Paliwal B, Ramesh KT, McCauley JW. Direct observation of the dynamic compressive failure of a transparent polycrystalline ceramic (AlON). J Am Ceram Soc 2006;89:2128–33.
[3] Grady DE, Kipp ME. Continuum modeling of explosive fracture in oil-shale. Int J Rock Mech Min 1980;17:147–57.
[4] Asay JR, Chhabildas LC. Reshock and release behavior of 6061-T6 aluminum. Bull Am Phys Soc 1980;25:566.
[5] Levy S, Molinari JF. Dynamic fragmentation of ceramics, signature of defects and scaling of fragment sizes. J Mech Phys Solids 2010;58:12–26.
[6] Bai YL, Dodd B. Adiabatic shear localization. 1st ed. Oxford: Pergamon Press; 1992.
[7] Stelly M, Legrand L, Dormeval R. Some metallurgical aspects of the dynamic expansion of shells. In: Meyers MA, Murr LE, editors. Shock waves and high-strain-rate penomena. New York: Plenum Press; 1981. p. 113–25.
[8] Grady DE. Shock deformation of brittle solids. J Geophys Res 1980;85:913–24.
[9] Wu Y, Li HX, Liu ZY, Chen GL, Lu ZP. Interpreting size effects of bulk metallic glasses based on a size-independent critical energy density. Intermetallics 2010;18:157–60.
[10] Raghavan R, Murali P, Ramamurty U. Ductile to brittle transition in the $Zr_{41.2}Ti_{13.75}Cu_{12.5}Ni_{10}Be_{22.5}$ bulk metallic glass. Intermetallics 2006;14:1051–4.
[11] Schuh C, Hufnagel T, Ramamurty U. Mechanical behavior of amorphous alloys. Acta Mater 2007;55:4067–109.
[12] Trexler MM, Thadhani NN. Mechanical properties of bulk metallic glasses. Prog Mater Sci 2010;55:759–839.
[13] Song SX, Nieh TG. Direct measurements of shear band propagation in metallic glasses – an overview. Intermetallics 2011;19:1968–77.
[14] Liu YH, Liu CT, Gali A, Inoue A, Chen MW. Evolution of shear bands and its correlation with mechanical response of a ductile $Zr_{55}Pd_{10}Cu_{20}Ni_5Al_{10}$ bulk metallic glass. Intermetallics 2010;18:1455–64.
[15] Greer AL, Cheng YQ, Ma E. Shear bands in metallic glasses. Mater Sci Eng R 2013;74:71–132.
[16] Dai LH. Shear banding in bulk metallic glasses. In: Bai YL, Dodd B, editors. Adiabatic shear localization: frontiers and advances. Waltham: Elsevier; 2012. p. 311–61.
[17] Pan J, Chen Q, Liu L, Li Y. Softening and dilatation in a single shear band. Acta Mater 2011;59:5146–58.
[18] Tandaiya P, Ramamurty U, Narasimhan R. Mixed mode (I and II) crack tip fields in bulk metallic glasses. J Mech Phys Solids 2009;57:1880–97.
[19] Tandaiya P, Narasimhan R, Ramamurty U. On the mechanism and the length scales involved in the ductile fracture of a bulk metallic glass. Acta Mater 2013;61:1558–70.
[20] Subhash G, Dowding RJ, Kecskes LJ. Characterization of uniaxial compressive response of bulk amorphous Zr-Ti-Cu-Ni-Be alloy. Mater Sci Eng A 2002;334:33–40.
[21] Li H. Negative strain rate sensitivity and compositional dependence of fracture strength in Zr/Hf based bulk metallic glasses. Scr Mater 2003;49:1087–92.
[22] Martin M, Kecskes L, Thadhani NN. Dynamic compression of a zirconium-based bulk metallic glass confined by a stainless steel sleeve. Scr Mater 2008;59:688–91.
[23] Zhu ZD, Ma E, Xu J. Elevating the fracture toughness of $Cu_{49}Hf_{42}Al_9$ bulk metallic glass: effects of cooling rate and frozen-in excess volume. Intermetallics 2014;46:164–72.
[24] He Q, Cheng YQ, Ma E, Xu J. Locating bulk metallic glasses with high fracture toughness: chemical effects and composition optimization. Acta Mater 2011;59:202–15.
[25] Chen Y, Jiang MQ, Dai LH. Collective evolution dynamics of multiple shear bands in bulk metallic glasses. Int J Plast 2013;50:18–36.
[26] Jiang MQ, Dai LH. Shear-band toughness of bulk metallic glasses. Acta Mater 2011;59:4525–37.
[27] Jiang MQ, Wang WH, Dai LH. Prediction of shear-band thickness in metallic glasses. Scr Mater 2009;60:1004–7.
[28] Jiang MQ, Dai LH. On the origin of shear banding instability in metallic glasses. J Mech Phys Solids 2009;57:1267–92.
[29] Shao Y, Yao K, Li M, Liu X. Two-zone heterogeneous structure within shear bands of a bulk metallic glass. Appl Phys Lett 2013;103:171901.
[30] Grady DE. Properties of an adiabatic shear-band process zone. J Mech Phys Solids 1992;40:1197–215.
[31] Grady DE, Kipp ME. The growth of unstable thermoplastic shear with application to steady-wave shock compression in solids. J Mech Phys Solids 1987;35:95–118.
[32] Dai LH, Yan M, Liu LF, Bai YL. Adiabatic shear banding instability in bulk metallic glasses. Appl Phys Lett 2005;87:141916.
[33] Dai LH, Bai YL. Basic mechanical behaviors and mechanics of shear banding in BMGs. Int J Impact Eng 2008;35:704–16.
[34] Zhang Y, Stelmashenko NA, Barber ZH, Wang WH, Lewandowski JJ, Greer AL. Local temperature rises during mechanical testing of metallic glasses. J Mater Res 2007;22:419–27.
[35] Miracle DB, Concustell A, Zhang Y, Yavari AR, Greer AL. Shear bands in metallic glasses: size effects on thermal profiles. Acta Mater 2011;59:2831–40.
[36] Conner RD, Li Y, Nix WD, Johnson WL. Shear band spacing under bending of Zr-based metallic glass plates. Acta Mater 2004;52:2429–34.
[37] Zhang H, Maiti S, Subhash G. Evolution of shear bands in bulk metallic glasses under dynamic loading. J Mech Phys Solids 2008;56:2171–87.
[38] Zhang H, Subhash G, Maiti S. Local heating and viscosity drop during shear band evolution in bulk metallic glasses under quasistatic loading. J Appl Phys 2007;102:043519.
[39] Grady DE. Adiabatic shear failure in brittle solids. Int J Impact Eng 2011;38:661–7.
[40] Xu J, Ramamurty U, Ma E. The fracture toughness of bulk metallic glasses. Jom 2010;62:10–8.
[41] Stoica M, Eckert J, Roth S, Zhang ZF, Schultz L, Wang WH. Mechanical behavior of $Fe_{65.5}Cr_4Mo_4Ga_4P_{12}C_5B_{5.5}$ bulk metallic glass. Intermetallics 2005;13:764–9.
[42] Hufnagel TC, Jiao T, Li Y, Xing LQ, Ramesh KT. Deformation and failure of $Zr_{57}Ti_5CU_{20}Ni_8Al_{10}$ bulk metallic glass under quasi-static and dynamic compression. J Mater Res 2002;17:1441–5.
[43] Liu YH, Wang G, Wang RJ, Zhao DQ, Pan MX, Wang WH. Super plastic bulk metallic glasses at room temperature. Science 2007;315:1385–8.
[44] Johnson WL, Lu J, Demetriou MD. Deformation and flow in bulk metallic glasses and deeply undercooled glass forming liquids – a self consistent dynamic free volume model. Intermetallics 2002;10:1039–46.